

**Field Tests of INEEL Tube-wave Suppressor and LBNL
Borehole Seismic System at Richmond Field Station, February
2001**

Thomas M. Daley and Roland Gritto
Lawrence Berkeley National Laboratory
Report LBNL-49015

Short title:

Abstract. Field tests of LBNL's borehole seismic field system and INEEL's tube-wave suppressor were conducted at the University of California's Richmond field station (RFS). Three different acquisition geometries were used, Single well, Crosswell and VSP. Data were acquired both with and without the tube-wave suppressor allowing measurement of the change in tube-wave strength. The ratio of P-wave to tube-wave energy was used for analysis. Both crosswell and single well tests showed 9 to 11 dB of reduction in tube wave amplitude (relative to the P-wave). The VSP data (using a sledge hammer surface source) showed minimal change in the amplitude ratio. Other equipment tests compared source strength of piezoelectric sources and recorded single well vertical profiles of two wells at RFS.

1. Introduction

A series of equipment tests were conducted at the U.C. Richmond Field Station using LBNL's borehole seismic system and INEEL's tube-wave suppressor. The tests used wells EMNE and INJ-1 (Figure 1). Our purpose is to quantify the effectiveness of the TWS as deployed in LBNL's SWSI (single well seismic imaging) system. We attempted to duplicate all acquisition parameters with and without the TWS. The same source and sensors were used, and the same depths were recorded. Additionally, tests were recorded in crosswell and Vertical Seismic Profile (VSP) type geometries.

To compare amplitudes of different arrivals, we use a moving window RMS amplitude analysis which is in the FOCUS-3D seismic processing software suite. This analysis calculates the value $E(t)$ for a time window: $E(t) = \sqrt{[f(t)^2 + H(f(t))^2]}$ where $f(t)$ is the recorded data and $H(f(t))$ is the Hilbert transform of the recorded data. The time window was 11 samples (1.375 ms) unless otherwise noted. By comparing the ratio of P-wave to tube-wave amplitude, we attempt to reduce the effect of source radiation pattern, depth dependent statics and other variables.

The tube-wave suppression tests are summarized in Table 1 along with the measured reduction in the ratio of tube-wave to P-wave amplitude.

Table 1.

Acquisition Geometry	Source	Receiver	Amplitude Ratio Improvement
SWSI	POV	OYO Hydrophones	11 dB
SWSI	POV	3-C Geophones	8 dB
XWell	LBNL Piezo	ITI Hydrophones	9 dB
XWell	LBNL Piezo	3-C Geophones	?
VSP	P Hammer	OYO Hydrophones	1 dB
VSP	S Hammer	OYO Hydrophones	-2 dB

2. Single Well

Figure 2 shows LBNL's single well equipment configuration with the INEEL TWS placed between the source and the top sensor. Figure 3 is a photo of the TWS as deployed above a well at a different site. In tests without the TWS, the sensors are attached to the borehole digitizer (A/D). The initial test used single well configurations with LBNL's POV source placed at 65 ft. depth in well EMNE. Figure 4 shows the recorded shot gather data with (left) and without (right) the TWS. There is a time delay of about 2 ms in the data with TWS because of the extra distance between source and receivers (eg. for channel 3, the first negative trough is at 21 ms with the TWS and at 19 ms without the TWS). This time varies with the surrounding material velocity. A reduction in tube-wave amplitude (between 40 and 80 ms) is observable on all channels.

Figure 5 is a plot of this amplitude analysis for a selected single well hydrophone

recording (channel 10) showing the amplitude of an 11 sample moving window in dB. The maximum amplitude of each trace (annotated as 0 dB on the figure) shows a total reduction of over 5 times the maximum amplitude (0.81 without TWS vs 0.15 with TWS). More importantly, the maximum energy is from the P-wave, rather than the tube-wave, when using the TWS. The ratio of P-wave to tube-wave energy is increased by 11 dB (from -2 dB without TWS to +9 dB with TWS).

3. Crosswell

Comparison seismograms for the crosswell tests are shown in Figure 6. In these tests the TWS was in the receiver borehole (EMNE) while the source was in INJ-1 (see Figure 1). The P-wave is the first arrival (13 to 17 ms) and the tube-wave is the second, larger amplitude arrival (17 to 28 ms). Again, the arrival times differ between the with and without tests because of different sensor depths. While a number of source depths were acquired, the shallower depths generated a larger tube-wave. The data in Figure 6 is for a source depth of 100 ft. Figure 7 shows the gain analysis for trace number 4 (channel 6). Again the amplitude of all arrivals has been reduced (from a maximum of 0.11 to 0.08) by the addition of the TWS. The ratio of P-wave to tube-wave maximum is increased from -12 dB to -3 dB; an increase of 9 dB when using the TWS.

4. Hammer VSP

Two data sets were collected by using a sledge hammer on the surface for a source and the single well configuration for sensors, giving an acquisition geometry identical

to vertical seismic profiles. One data set used the standard P-wave type source, ie. the hammer hitting a flat plate on the ground. The second data set used an S-wave type source, ie. a wood plank held down by a vehicle and struck on its vertical side. The plank was aligned toward the well, giving an in-line S-wave source. The recording system triggering did not work correctly for the VSP acquisition, so a zero time pulse was recorded on Channel 1, as shown with the seismograms. Times are relative to this zero time pulse. For ease of comparison, we have chosen recordings whose zero time was approximately equal. Figure 8 shows the P-wave VSP seismograms. The observable arrival is the tube wave. Figure 9 shows the amplitude analysis averaged for 4 traces (sequentially traces 3 to 6). In this case the improvement in P-wave to tube-wave ratio is only 1 dB (from -16dB to -15 dB).

Figure 10 shows seismograms for the S-wave VSP test, and Figure 11 shows the amplitude analysis. The identification of arrivals is more difficult in this data set, however we believe a small P-wave at about 20 ms is followed by a larger S-wave at about 25 ms and the tube-wave at about 35 ms. The ratio of P-wave to tube-wave is actually reduced about 2 dB while the S-wave to tube-wave ratio is a constant 3 dB. It is unclear at this time why the TWS did not perform well in this acquisition geometry. However, the VSP data was the poorest in terms of body-wave signal-to-noise ratio and we may be misidentifying wave types.

5. Single Well with Clamping Geophones

In most cases, recording 3-component single well data is optimal, albeit more expensive. For this reason we also tested the TWS with our wall-locking 3-component borehole geophone sensors using the piezoelectric POV source. A single well shot gather with and without TWS is shown in figure 12; as before the arrival times are slightly delayed with the TWS because of increased source-receiver spacing. A clear reduction in tube-wave energy is observed. The amplitude analysis of this data set is shown in Figure 13. We see a reduction in maximum amplitude from 0.092 to 0.0066, with a reduction in tube-wave to P-wave ratio of 8 dB (-16 dB to -8 dB).

It is notable that for the geophone testing we were able to place a geophone between the TWS and the source. This data (channels 3, 4 and 5 in Figure 12) has a gain analysis shown in figure 14. Unfortunately, the P-wave arrival is superimposed on the low-frequency tube-wave arrival, so amplitude interpretation in the time-domain is difficult. Comparing the maximum amplitude (over an 11 sample window) for channel 3 (trace 1 in Figure 12, the vertical component above the TWS) to channel 6 (trace 4 in Figure 12, the vertical component below the TWS) we have $0.76 / 0.13 = 5.8$; without the TWS the ratio is $1.1 / 0.91 = 1.21$. It is surprising that the geophone above the TWS sees a reduction in amplitude, however the reduction in ratio is indicating a 13.6 dB decrease in tube-wave energy.

5.1. Spectral Analysis

Spectral analysis of a 16 ms time window (128 samples) with a 1 ms (8 sample) move up was used for time vs frequency analysis. In Figure 15 we look at spectral analysis of the "control" geophone (the top geophone, between the source and the TWS), we see a 5 dB drop in peak energy (at about 300 Hz), with an unexpected increase in relative energy between 700 and 1000 Hz with the TWS. Analysis of the wall-locking geophone data was hampered by large electrical cross-talk from the high voltage source pulse. Subsequent to data acquisition this problem was isolated and should not affect future acquisition. Extra data processing was applied to reduce the impact of the electrical cross-talk. A 3.5 ms mute was applied to the beginning of all recordings and a minimum phase Ormsby bandpass filter (250-3500 Hz) was applied. The direct P-wave arrival is difficult to identify because it is superimposed on the cross talk, however spectral analysis allows identification because the peak P-wave frequency at about 2400 Hz is significantly removed from the peak tube-wave frequency at about 200 Hz. Figure 16 shows the ratio of these two spectral peaks is -17 dB with the TWS and -23 dB without the TWS. We therefore see a 6 dB reduction in tube-wave/P-wave spectral power ratio, for all times.

Because the tube wave has more reverberant energy, we look to the contoured peaks in Figure 16 to get the tube-wave/P-wave ratio at the time window of peak energy. This analysis shows -6dB with the TWS and -18 dB without the TWS for a total improvement of 12 dB in signal-to-noise ratio.

Crosswell data was collected with the wall-locking geophones, however no identifiable tube-wave was recorded, either with or without the TWS.

6. Single Well Vertical Profiles (SWVP)

To better understand the wavefields and velocities of the wells used for this tube-wave suppression testing, we recorded SWVP data which has a fixed source at the bottom of the well and equally spaced sensors covering the well depth. We used the LBNL piezo source and our ITI (Innovative Transducers Inc.) 24 sensor hydrophone string with 0.5 m spaced sensors. The resulting data is shown in Figures 17 and 18 for wells EMNE and INJ-1, respectively. We see a significantly different wavefield with differing P-wave and tube-wave velocities and amplitudes. This data was used to confirm our interpretation of P-wave and tube-wave arrivals in the above crosswell and single well data analysis.

7. LBNL Piezoelectric Source Comparison

A comparison test of LBNL's piezo and POV sources was made using crosswell acquisition geometry. The POV source is used for single well and crosswell studies, while the LBNL piezo (SN# B) is one of many similar source currently used only for crosswell.

Figures 19 and 20 show amplitude and energy analysis using a variety of algorithms (included in the FOCUS-3D package) for 24 hydrophones (the ITI string) at 0.5 m spacing from 40.5 to 52 m in well INJ-1 for the LBNL piezo source (Figure 19) and

LBNL's POV source (Figure 20) at 45.7 m depth in well EMNE. Both sources had a 4 kV peak-to-peak input signal. We see that the LBNL piezo has slightly stronger output. The peak amplitude ratio is 1.35, while the energy ratio is 1.94. There are also some differences in individual channel responses, possibly indicating variation in source radiation patterns between sources.

8. Summary

We have observed a measurable reduction in tube-wave energy for both single well and crosswell acquisition geometries. This reduction is best quantified as the ratio of P-wave to tube-wave energy since there was an overall reduction in trace amplitudes. The ratio is reduced 8 to 11 dB in single well and crosswell geometries. No reduction was observed in the VSP hammer surveys; this is surprising and may be due to misidentification of body wave phases or to surface-wave/tube-wave interaction unique to surface sources. Since the primary import of this work is single well and crosswell surveys, we consider the 8-11 dB reduction seen in these geometries as a promising success. One notable field observation was that the TWS had a slight leak causing small air bubbles to be continuously released. Because we had an overall reduction in recorded body wave amplitudes (separate from the reduction of the tube-wave amplitudes), we believe that the constant presence of air bubbles in the water column led to an overall reduction in energy transmitted to the formation. We also note that the borehole diameter was 6 inches, while the TWS maximum diameter was about 5.25 inches. So the physical presence of a blockage in the well could account for some of

the tube-wave reduction in the form of reflected tube-waves. The test with a clamped geophone above the TWS was the only one to avoid this effect and this test did show a reduction in tube-wave energy. We therefore conclude that the INEEL TWS is effective in suppressing borehole tube-wave energy.

9. Acknowledgements

This work was supported by the Assistant Secretary for Fossil Energy, Office of Natural Gas and Petroleum Technology, through the National Petroleum Technology Office, Natural Gas and Oil Technology Partnership. Processing was performed at the Center for Computational Seismology, which is supported by the Director, Office of Science, Office of Basic Energy Sciences, Division of Engineering and Geosciences, of the U.S. Department of Energy under Contract No. DE-AC03-76SF00098.

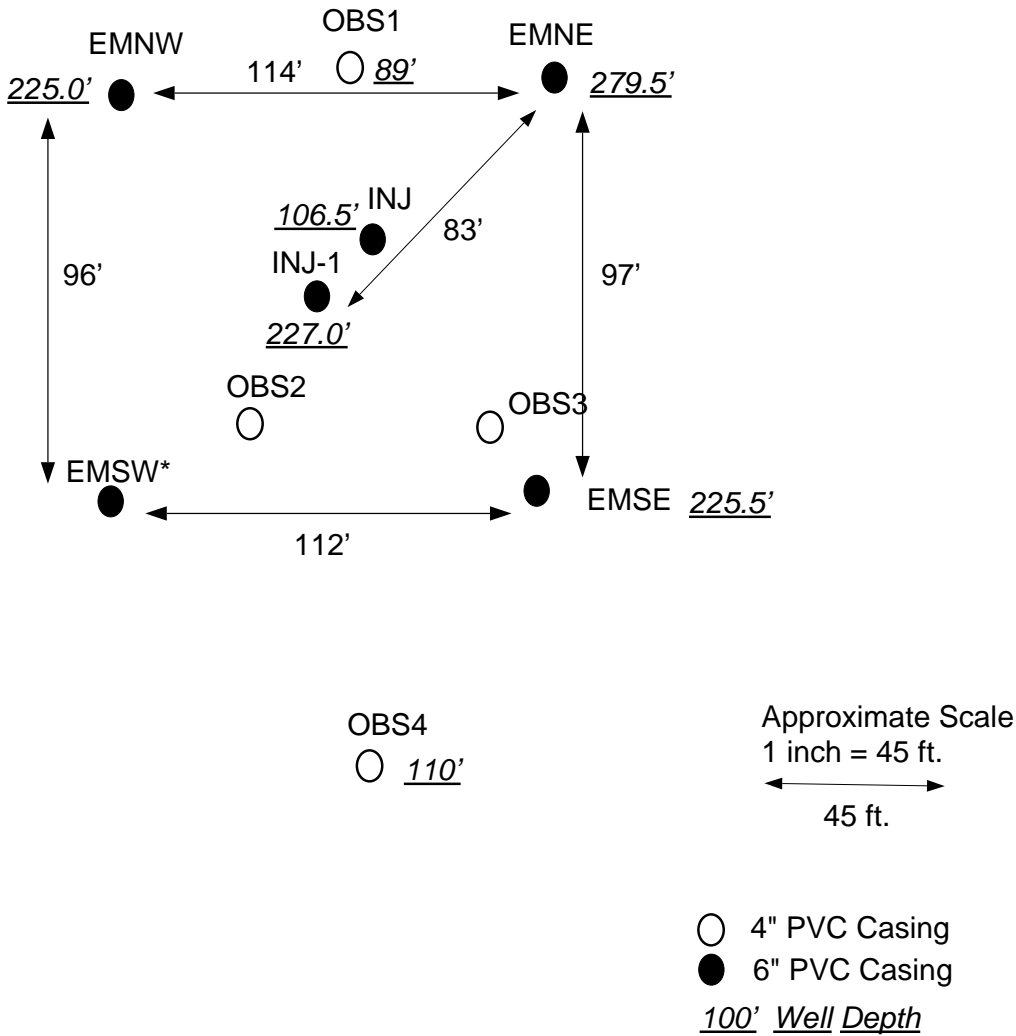
10. Disclaimer

This document was prepared as an account of work sponsored by the United States Government. While this document is believed to contain correct information, neither the United States Government nor any agency thereof, nor The Regents of the University of California, nor any of their employees, makes any warranty, express or implied, or assumes any legal responsibility for the accuracy, completeness, or usefulness of any information, apparatus, product, or process disclosed, or represents that its use would not infringe privately owned rights. Reference herein to any specific commercial product, process, or service by its trade name, trademark, manufacturer, or otherwise, does not

necessarily constitute or imply its endorsement, recommendation, or favoring by the United States Government or any agency thereof, or The Regents of the University of California. The views and opinions of authors expressed herein do not necessarily state or reflect those of the United States Government or any agency thereof, or The Regents of the University of California.

Ernest Orlando Lawrence Berkeley National Laboratory is an equal opportunity employer.

Richmond Field Station - Borehole Test Site



Note: 6" PVC Casing -> O.D.=6.5", I.D.= 5.75"

Note: All water levels 7 - 9 ft. (Feb, 2001)

* Well EMSW has a seismometer permanently emplaced.

Figure 1. Location map for RFS wells.

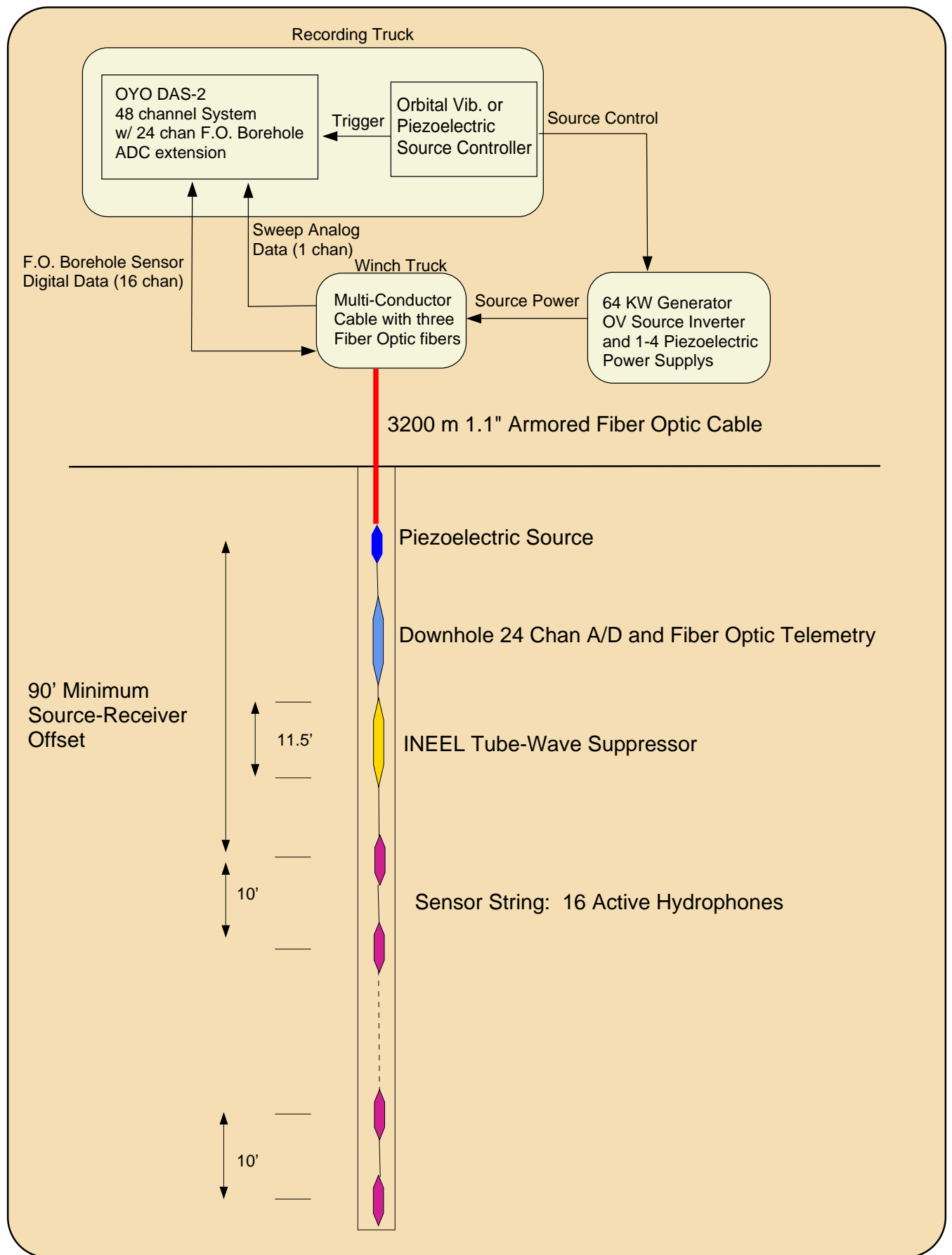


Figure 2 LBNL single well seismic imaging system with INEEL tube-wave suppressor.

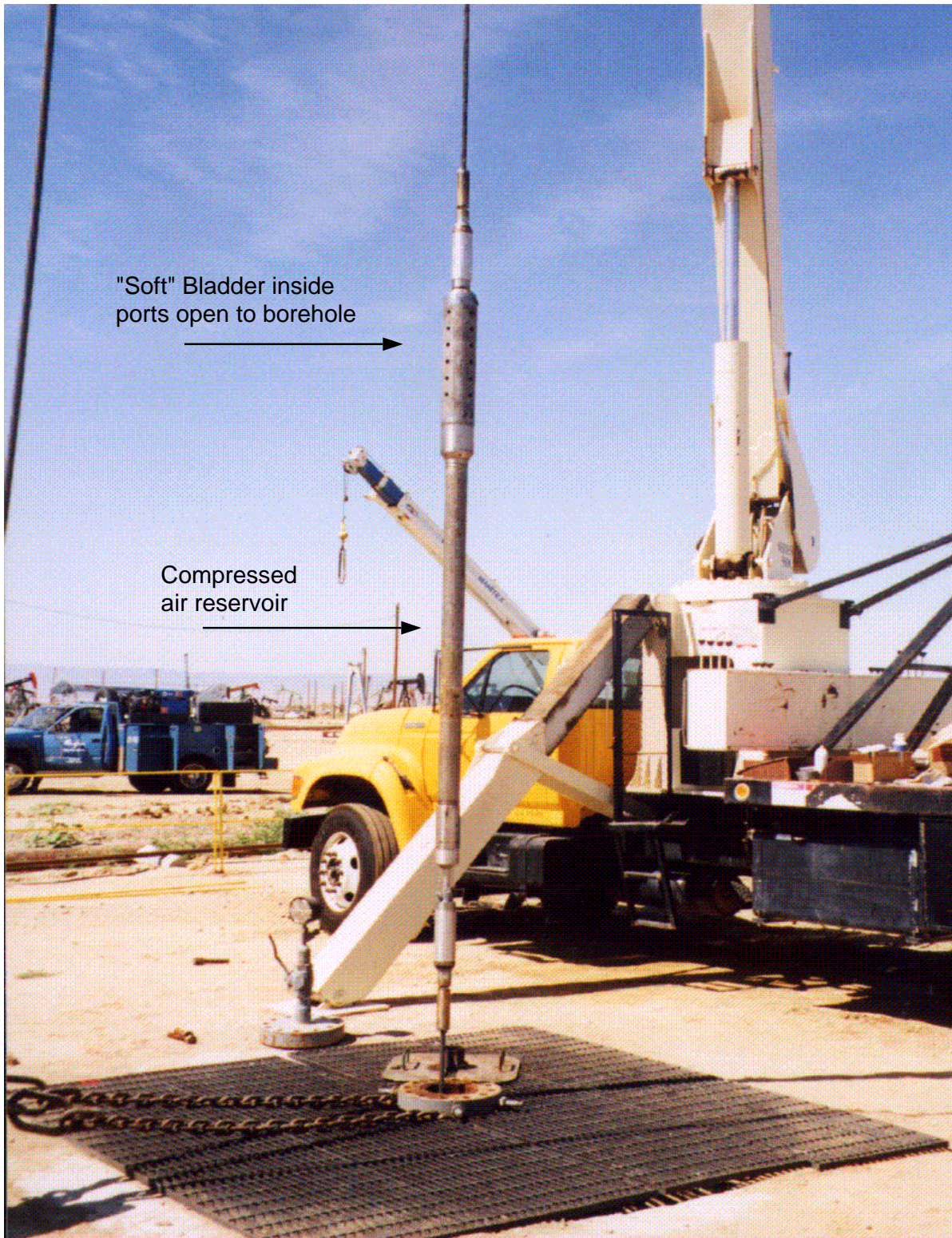


Figure 3. INEEL tube-wave suppressor deployed as part of LBNL's single well seismic equipment.

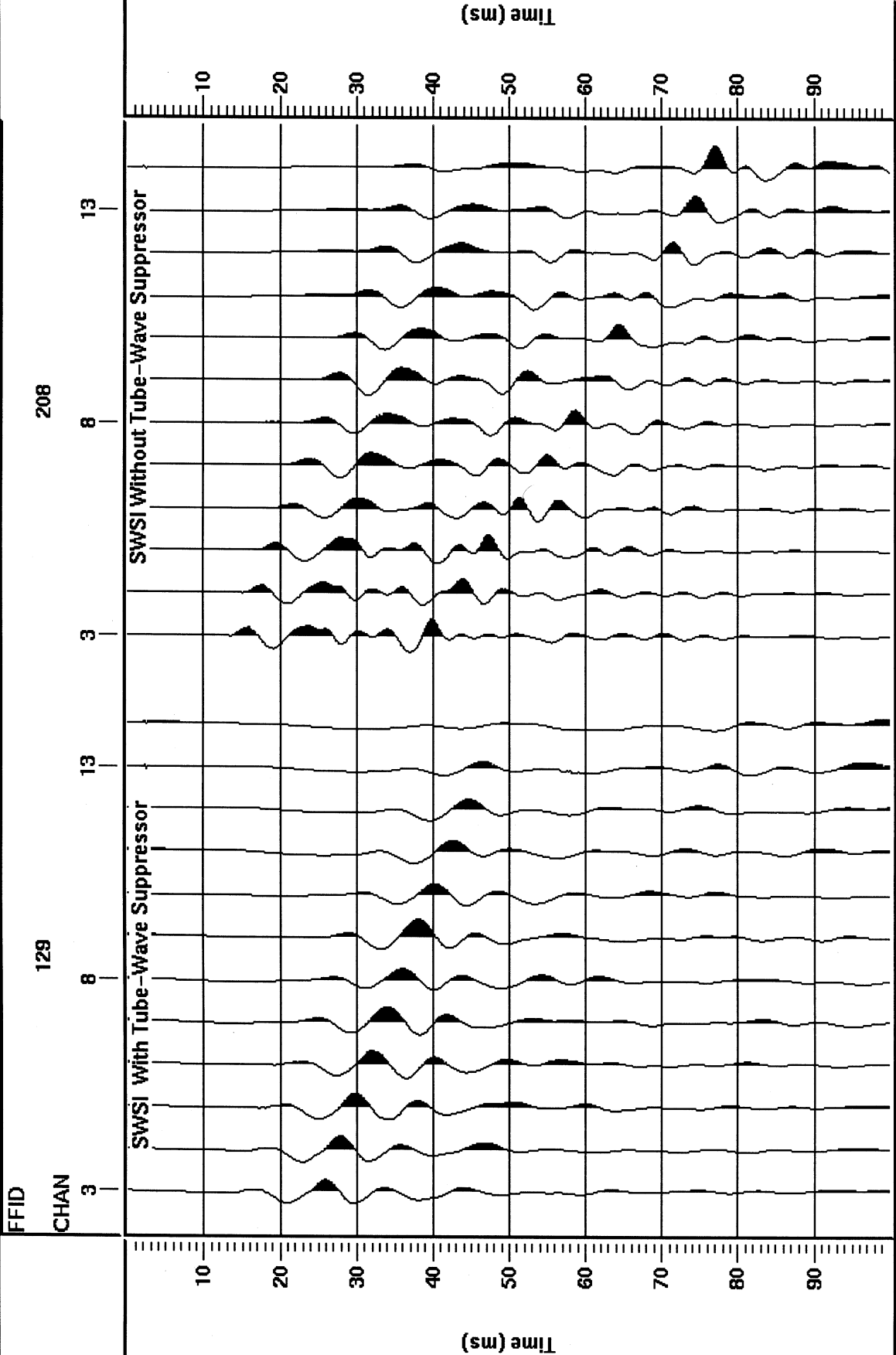


Figure 4. Comparison of seismograms for single well data recorded with (left) and without (right) the INEEL tube-wave suppressor.

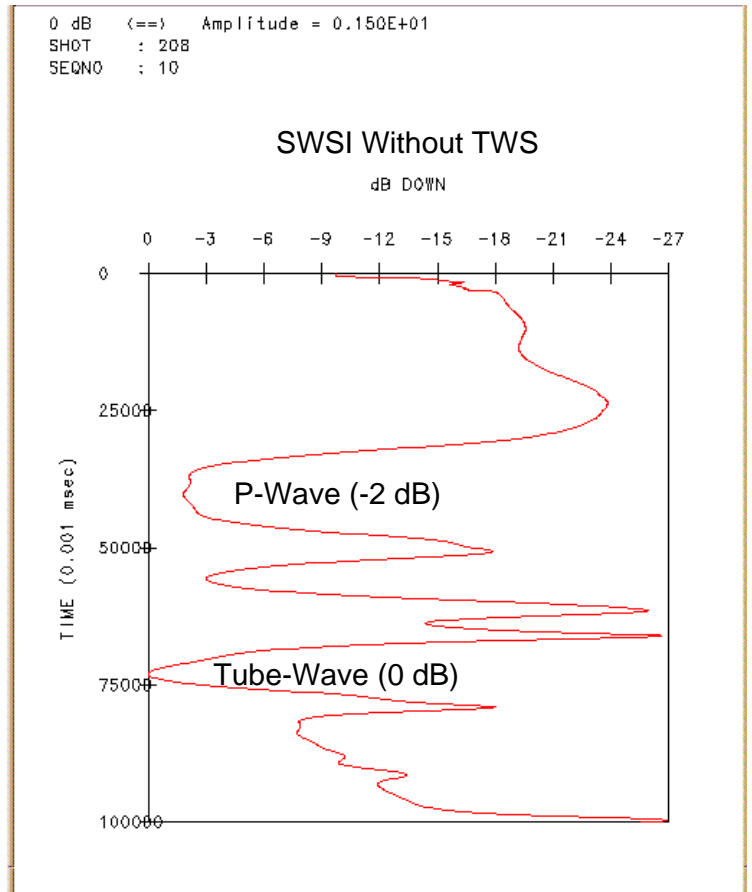
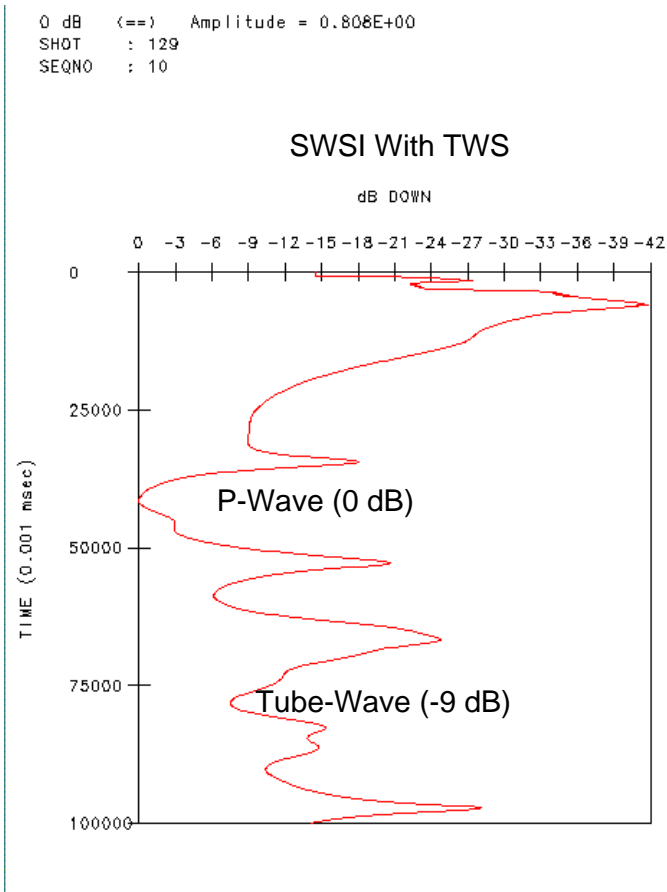


Figure 5. Amplitude vs time comparison for single well data recorded with TWS (left) and without TWS (right). The improvement in P-wave to tube-wave amplitude ratio is 11 dB.

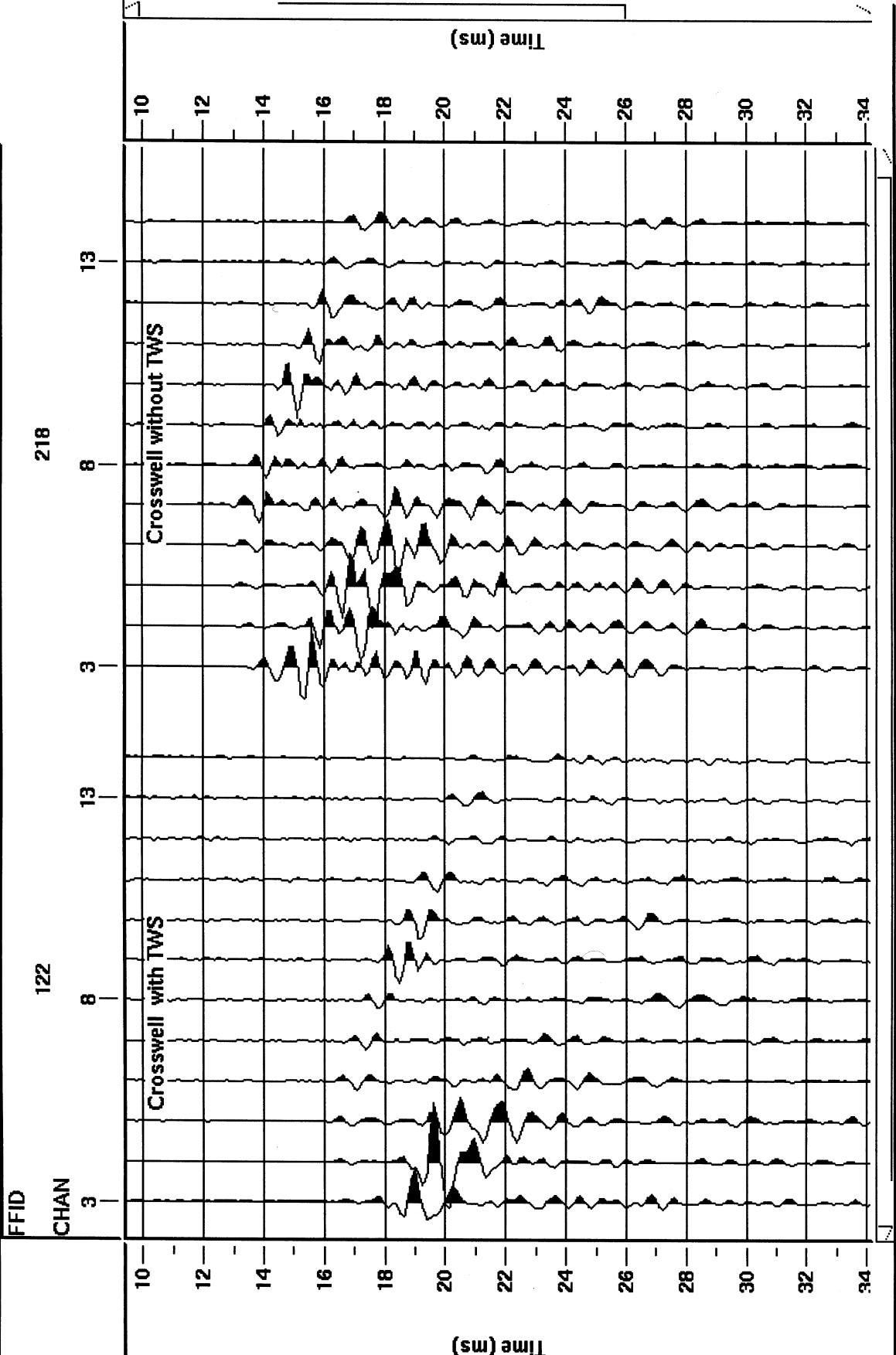


Figure 6. Comparison of seismograms for crosswell data recorded with (left) and without (right) the INEEL tube-wave suppressor.

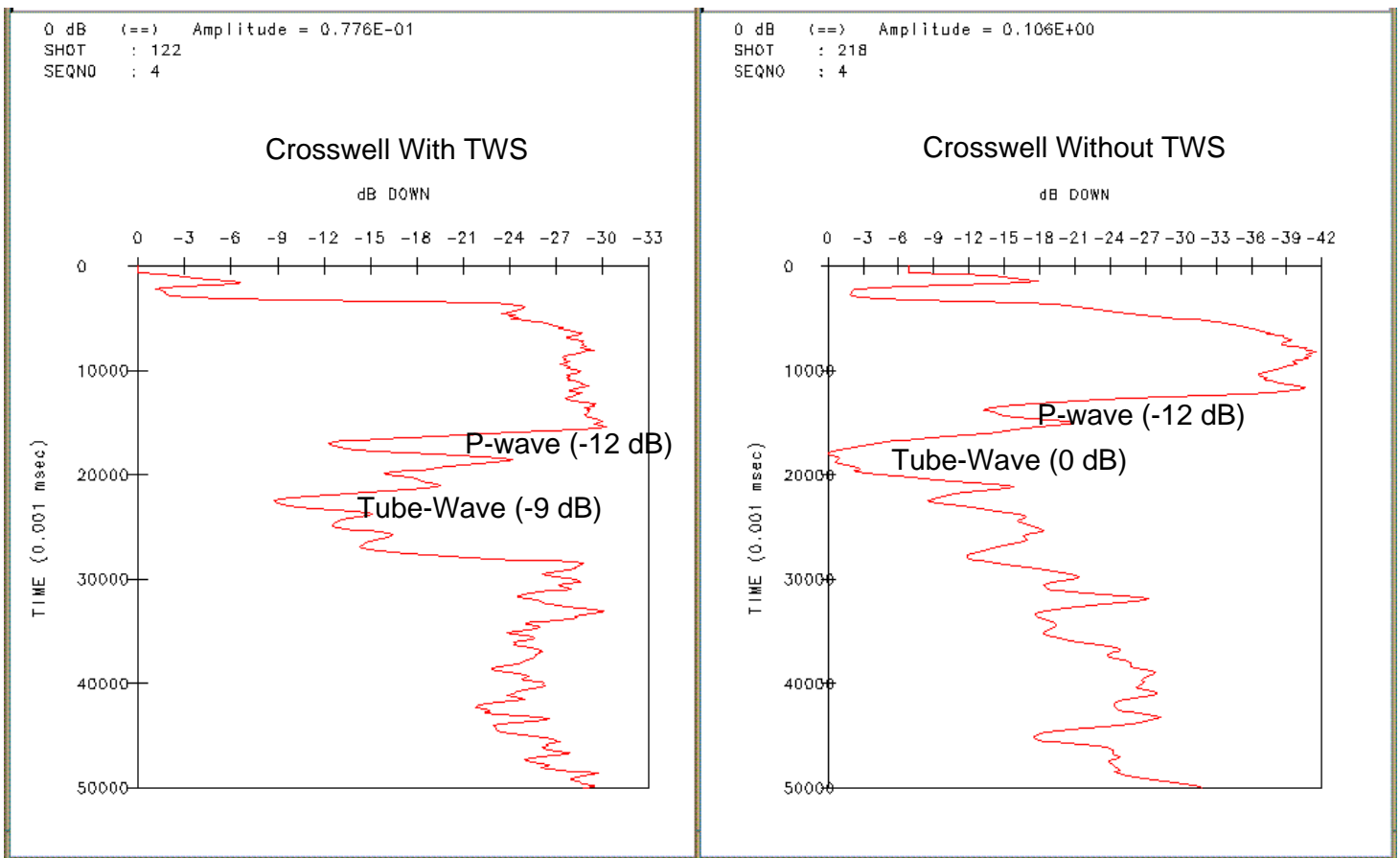


Figure 7. Amplitude vs time comparison of crosswell data recorded with TWS (left) and without TWS (right). The improvement in the ratio of P-wave to tube-wave energy is 9 dB.

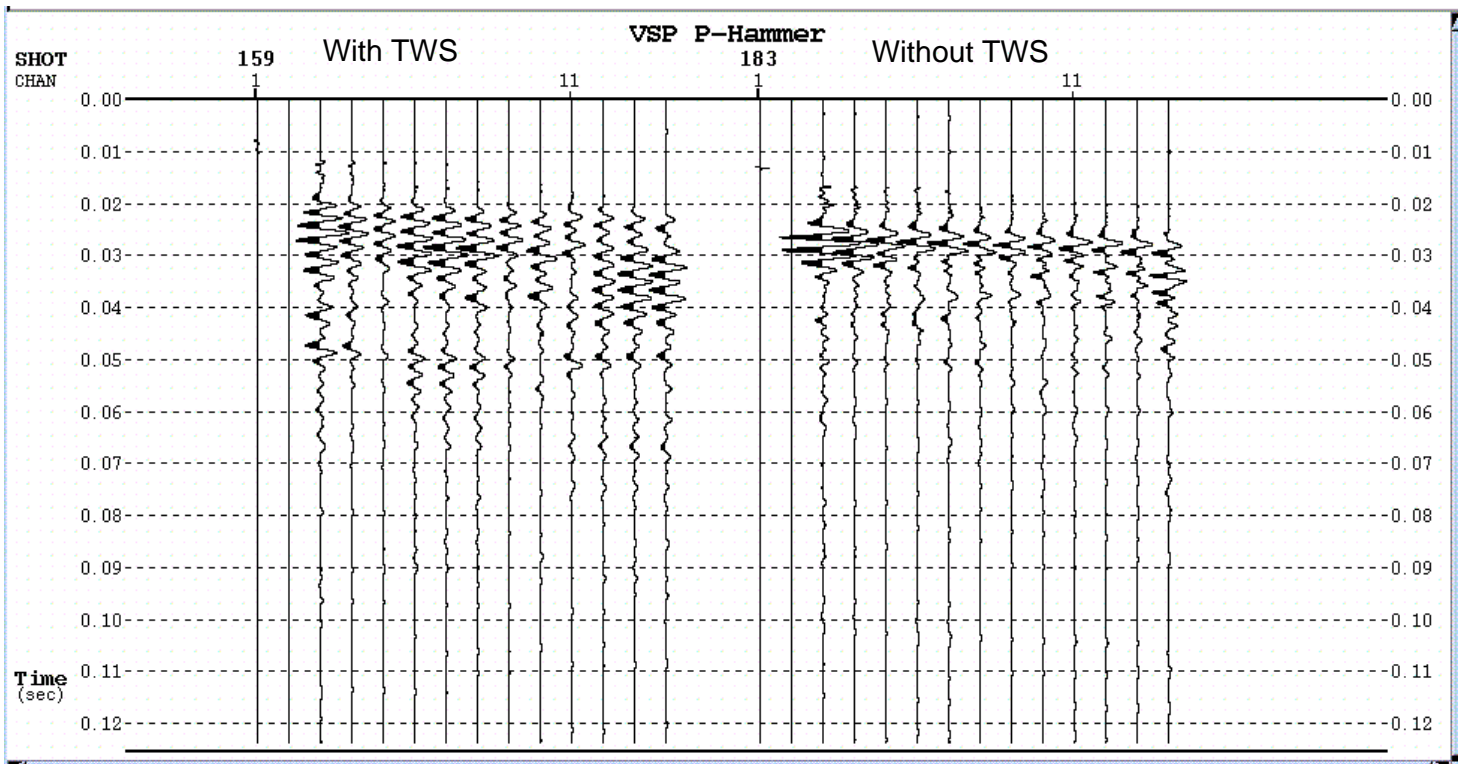


Figure 8. Data traces from a sledge hammer source VSP (P-wave mode) acquired with TWS (left) and without TWS (right). The tube-wave is the arrival between 20 and 40 ms.

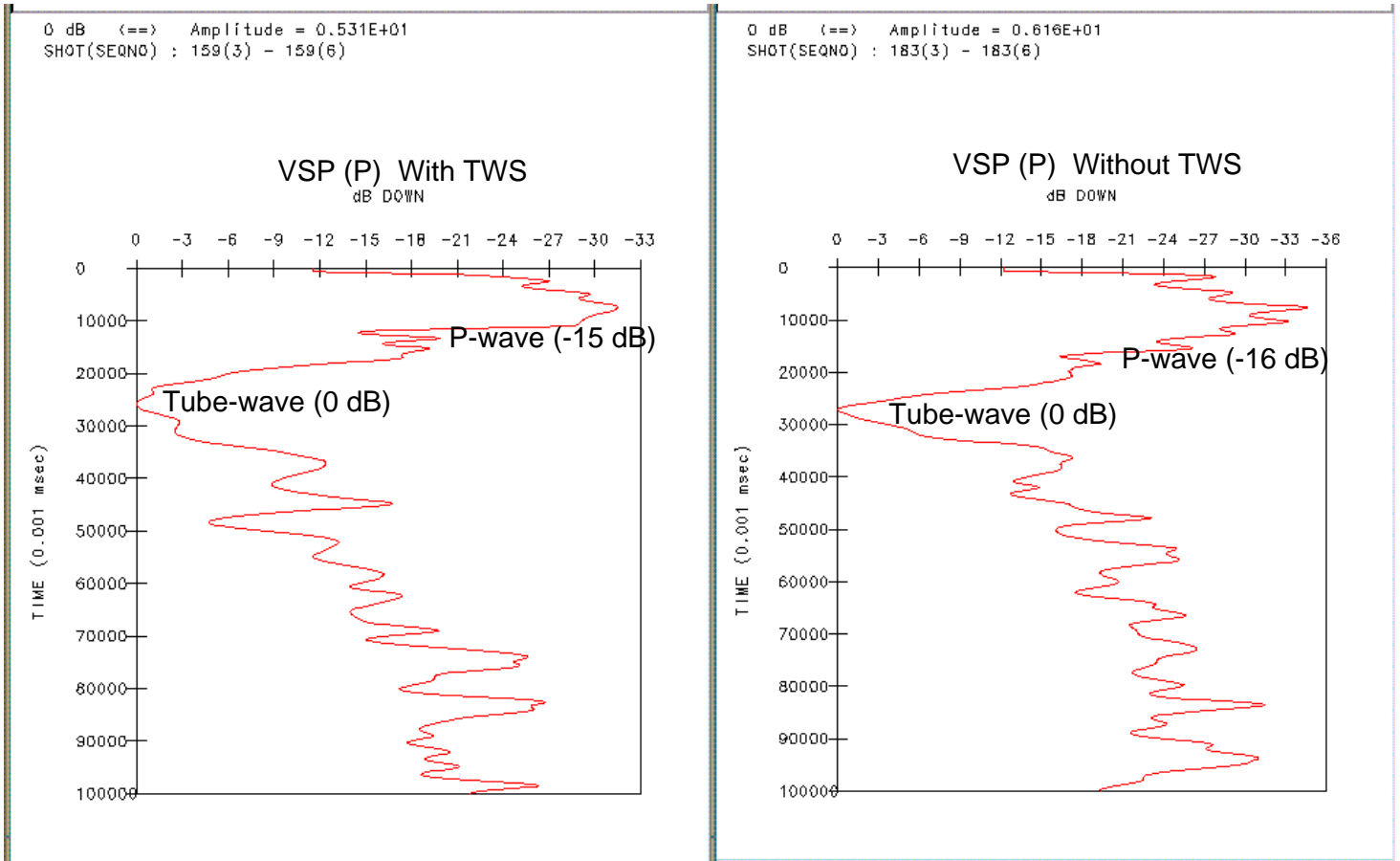


Figure 9. Amplitude vs time comparison of VSP data recorded with (left) and without (right) the INEEL tube-wave suppressor. The improvement in P-wave to tube-wave amplitude ratio is 1 dB.

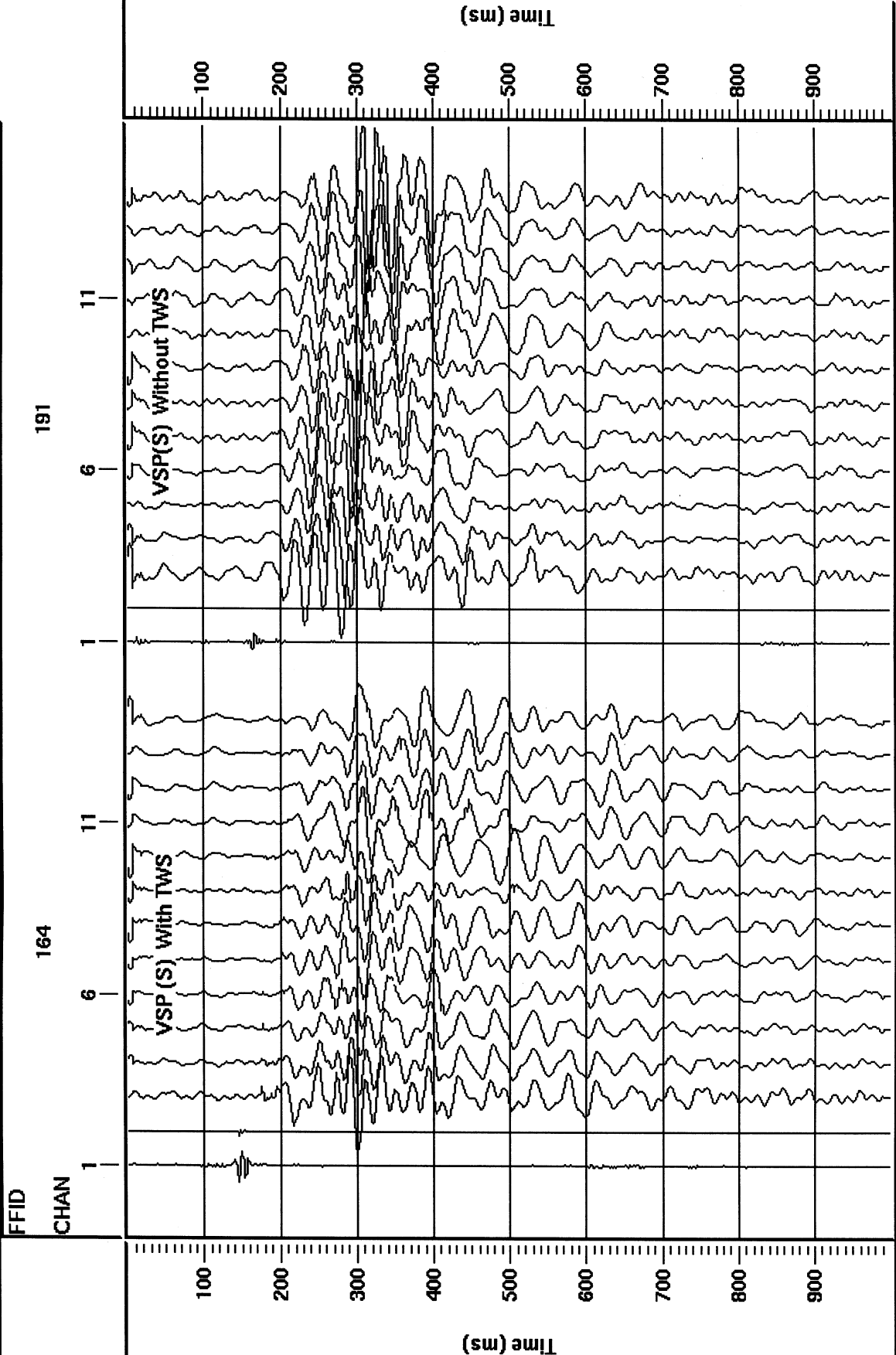


Figure 10. Comparison of seismograms for S-wave hammer VSP data recorded with (left) and without (right) the INEEL tube-wave suppressor.

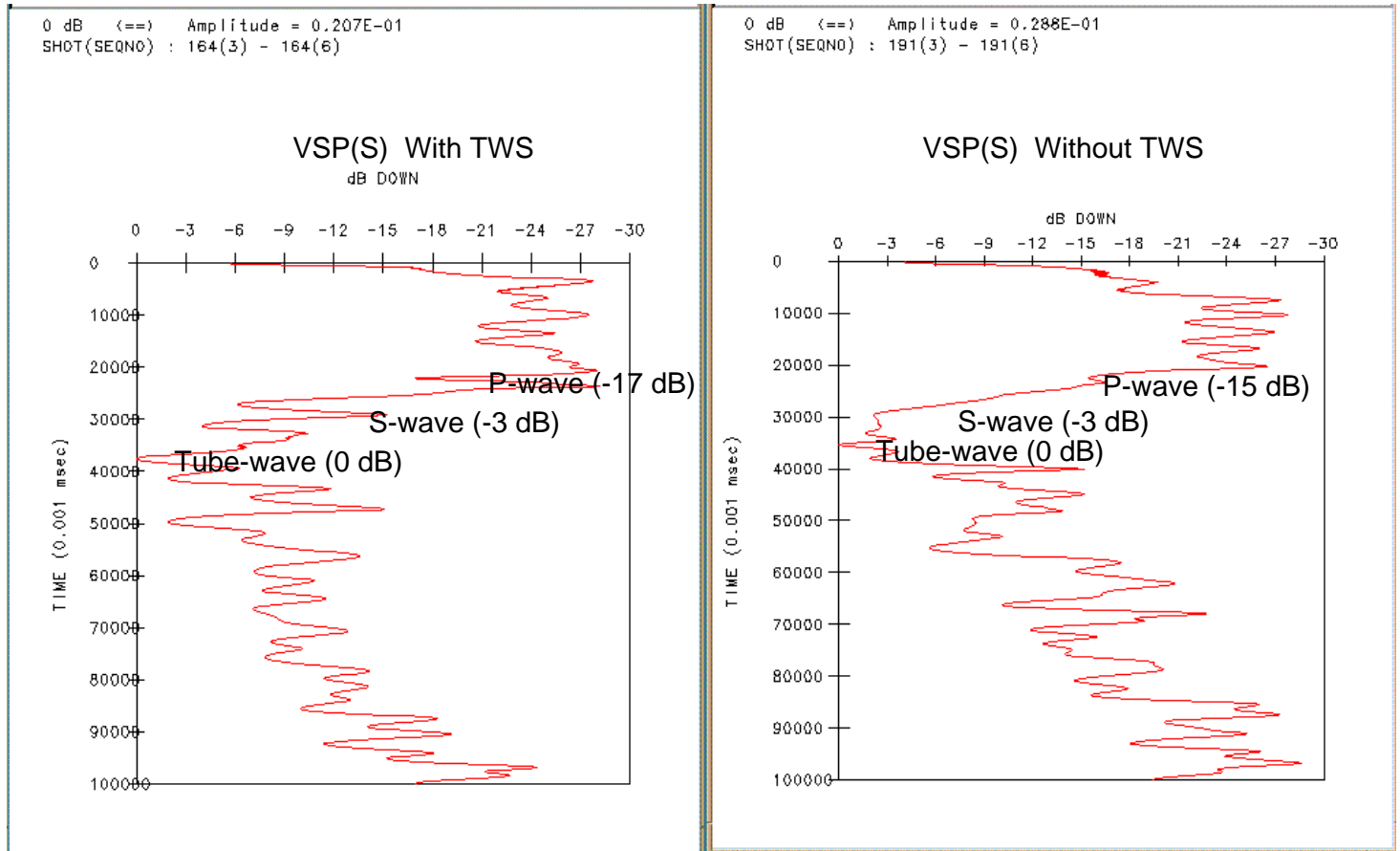


Figure 11. Amplitude vs time analysis for VSP data recorded with an S type hammer source both with (left) and without (right) the INEEL tube-wave suppressor. The ratio of S-wave to tube-wave amplitudes is unchanged.

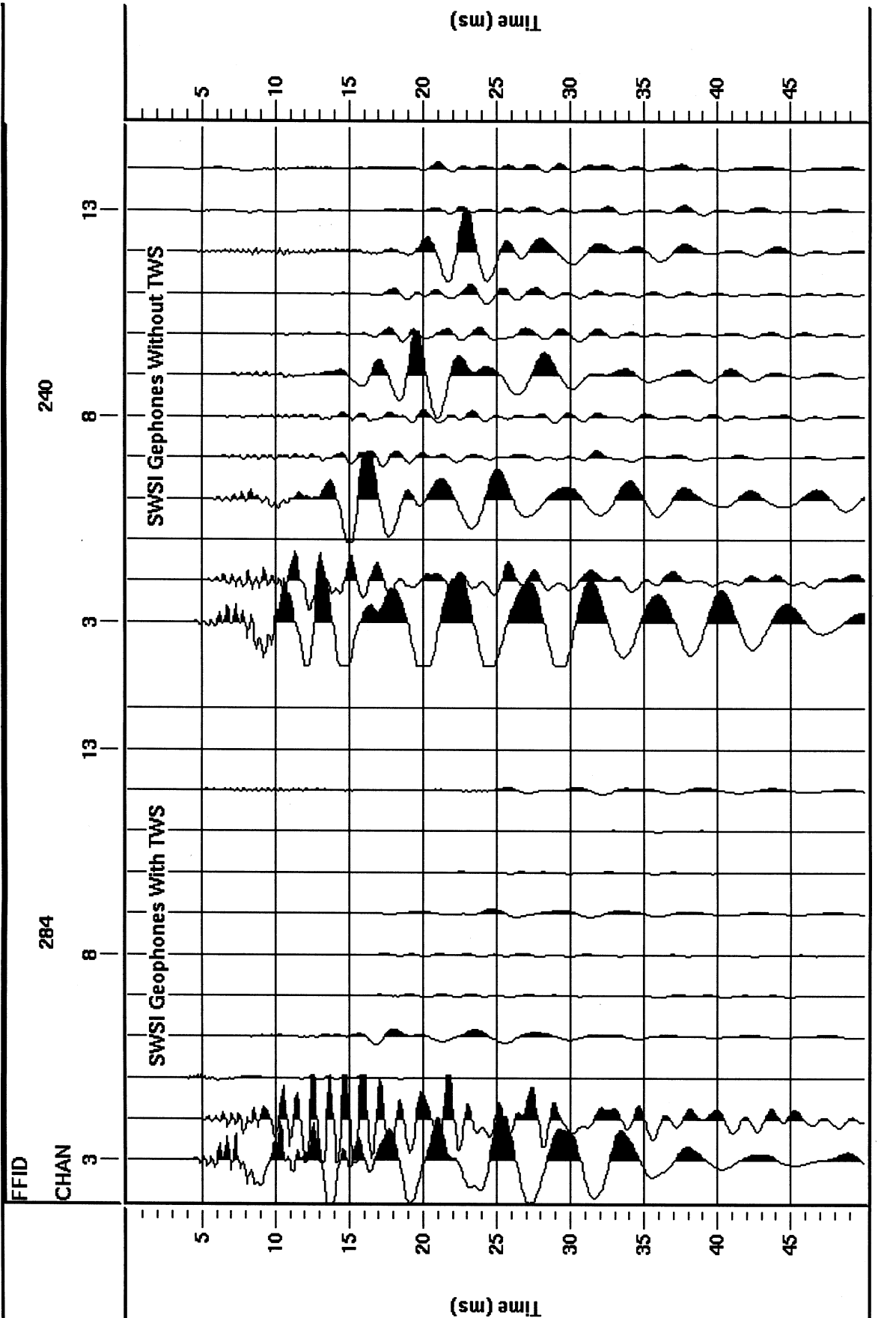


Figure 12. Comparison of seismograms for single well 3-component geophone data recorded with (left) and without (right) the INEEL tube-wave suppressor.

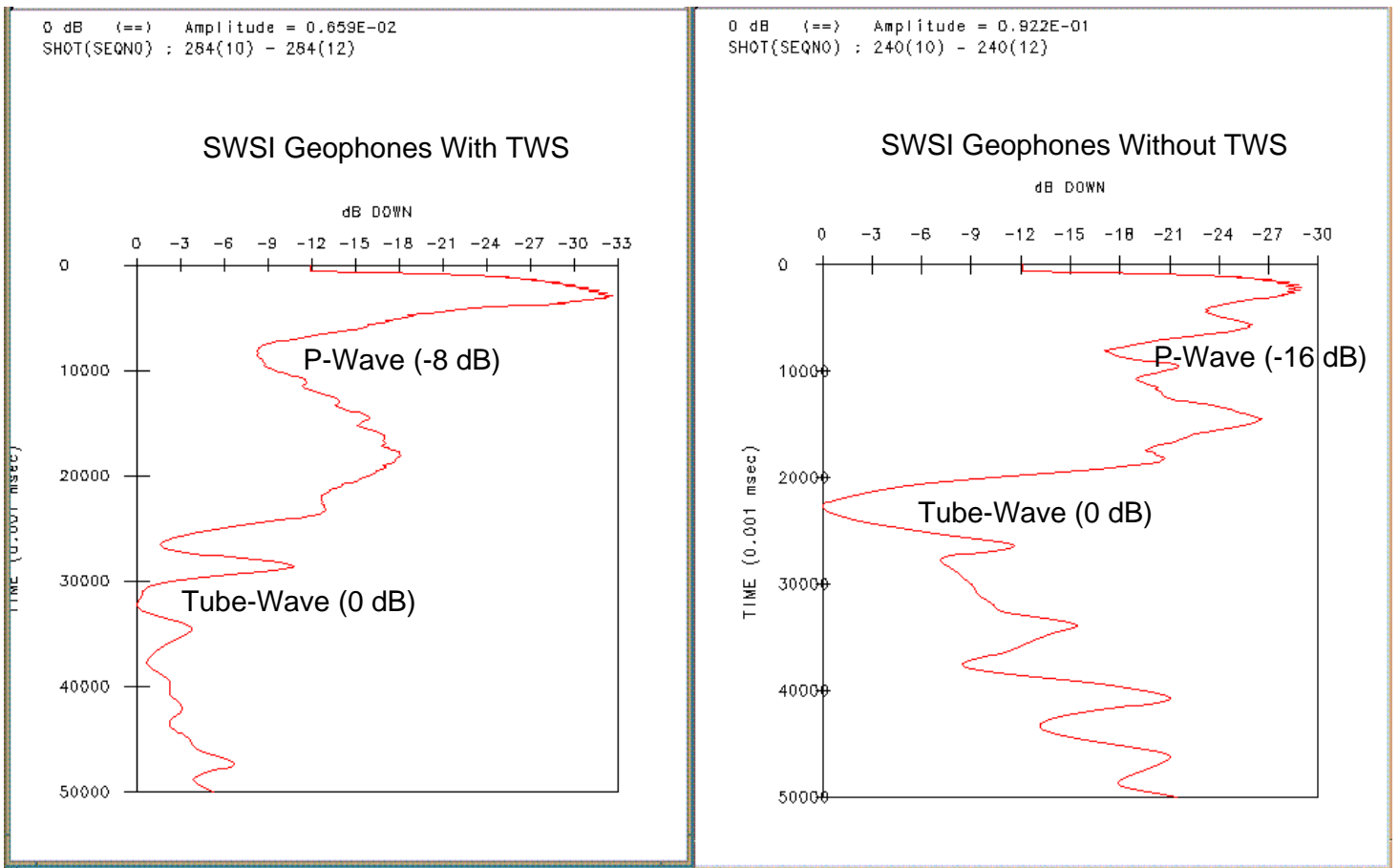


Figure 13. Amplitude vs time analysis for single well data recorded with wall-locking geophones both with (left) and without (right) the INEEL tube-wave suppressor. The improvement in P-wave to tube-wave amplitude ratio is 8 dB.

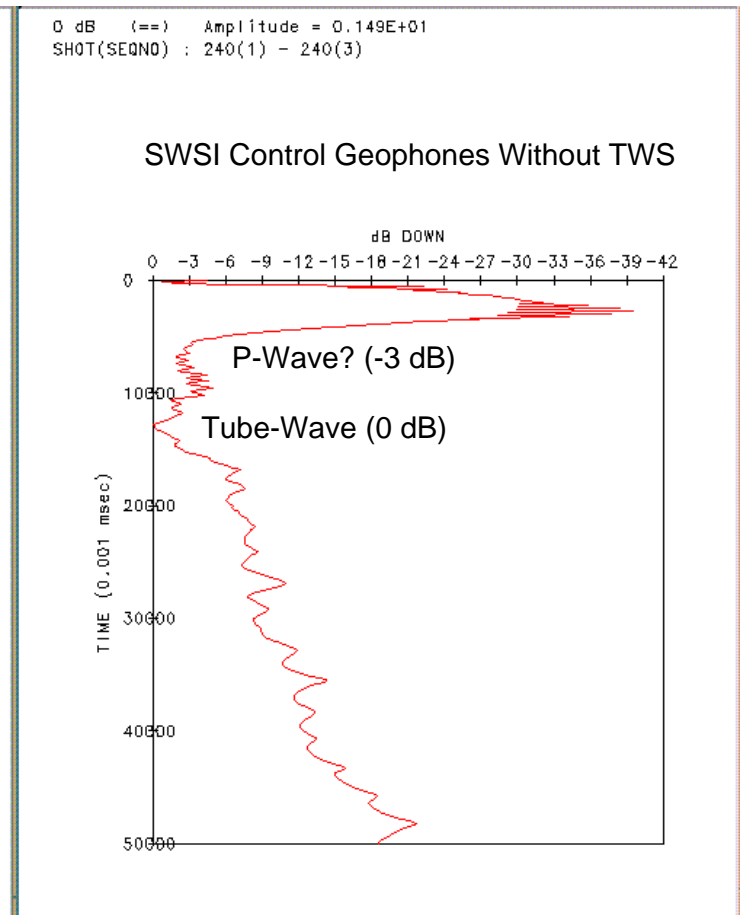
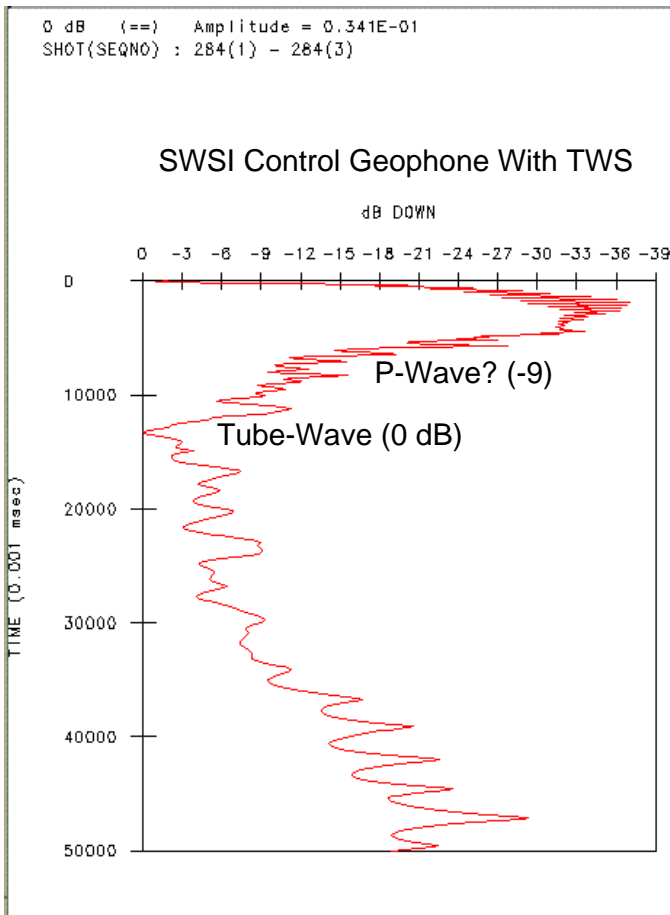


Figure 14. Amplitude vs time analysis of single well data recorded with a "control" geophone (one placed between the source and the TWS), both with (left) and without (right) the INEEL tube-wave suppressor. The P-wave is difficult to identify because the interval time between P and tube waves is small.

SWSI Control Geophone With TWS

SWSI Control Geophones Without TWS

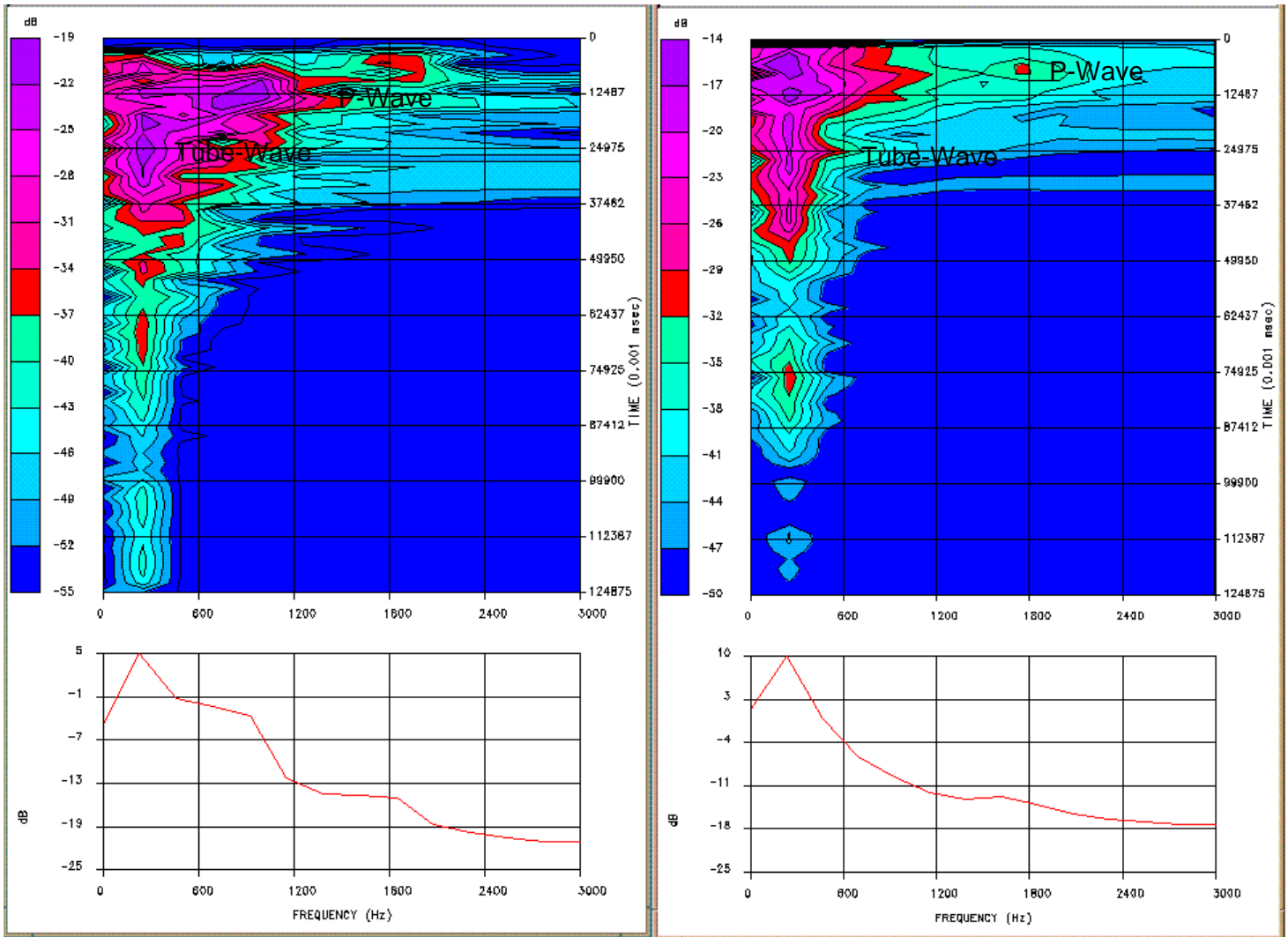


Figure 15. Frequency vs time analysis (top) and total spectral content (bottom) for single well data recorded with (left) and without (right) the INEEL tube-wave suppressor. We interpret a 5 dB improvement in the ratio of P-wave (at 1800 Hz) to tube-wave (at 250 Hz).

Spectral Analysis of Single Well Geophone Data

With TWS

Without TWS

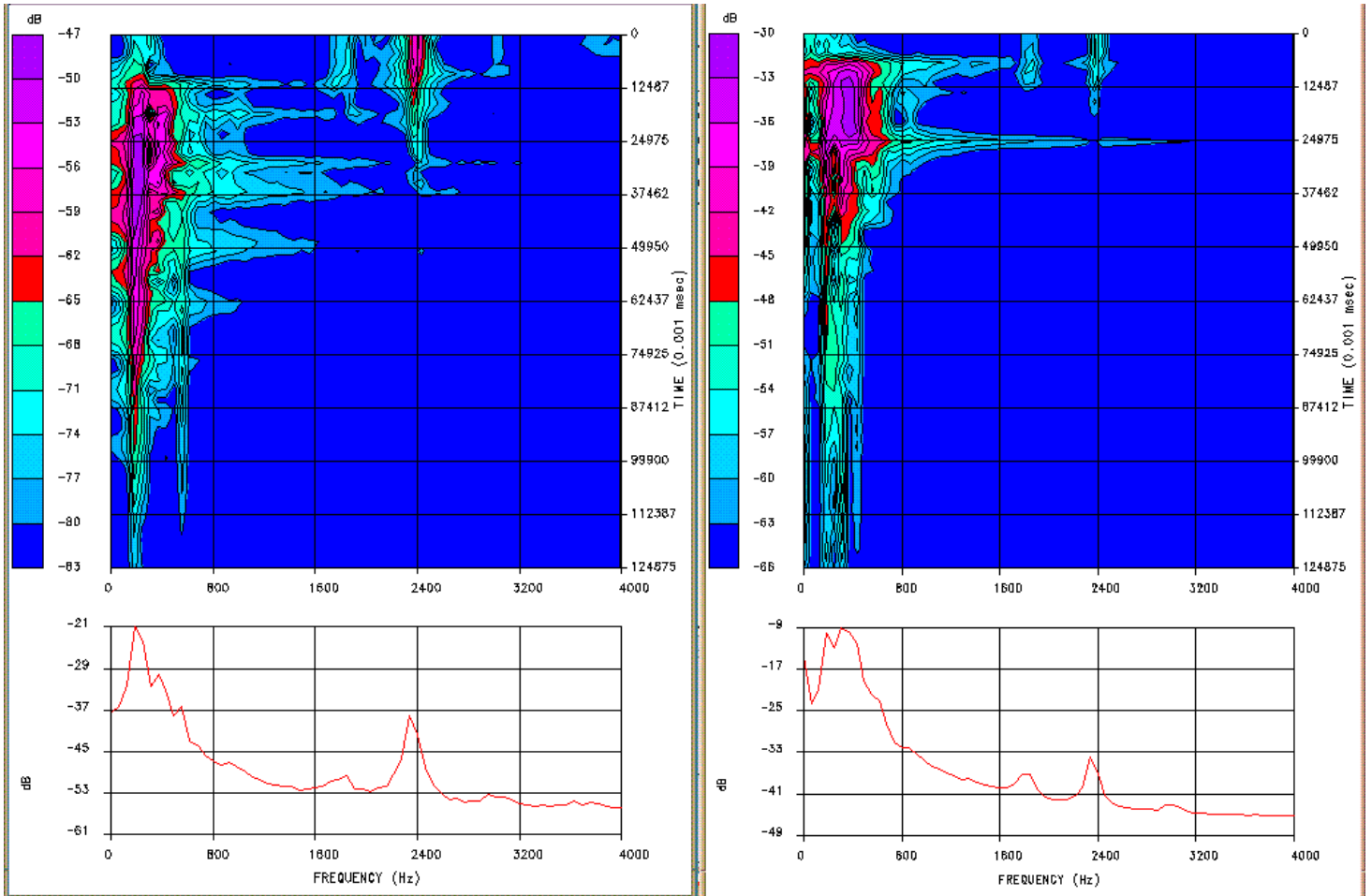


Figure 16. Spectral analysis of single well geophone data. Frequency vs time (top) and total spectra (bottom) are shown for a data recorded with the INEEL tube-wave suppressor (left) and without the TWS (right). The P-wave has a peak at 2400 Hz, while the tube wave has a spectral peak at about 200 -400 Hz.

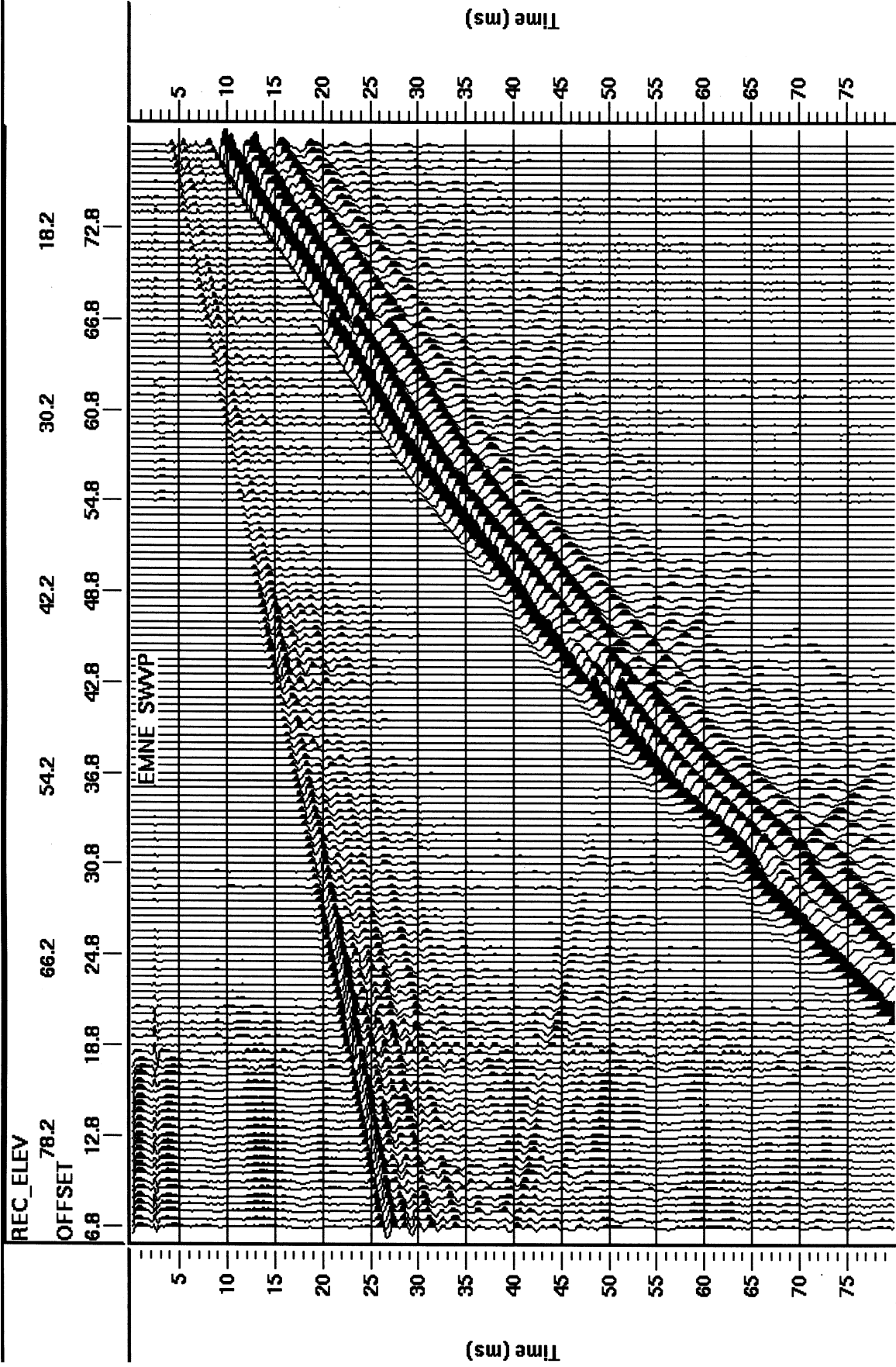


Figure 17. Single well vertical profile of well EMNE showing P-wave (5-25 ms) and tube-wave (10-75 ms). The receiver depth and source-receiver offset are labeled as rec_elev and offset, respectively.

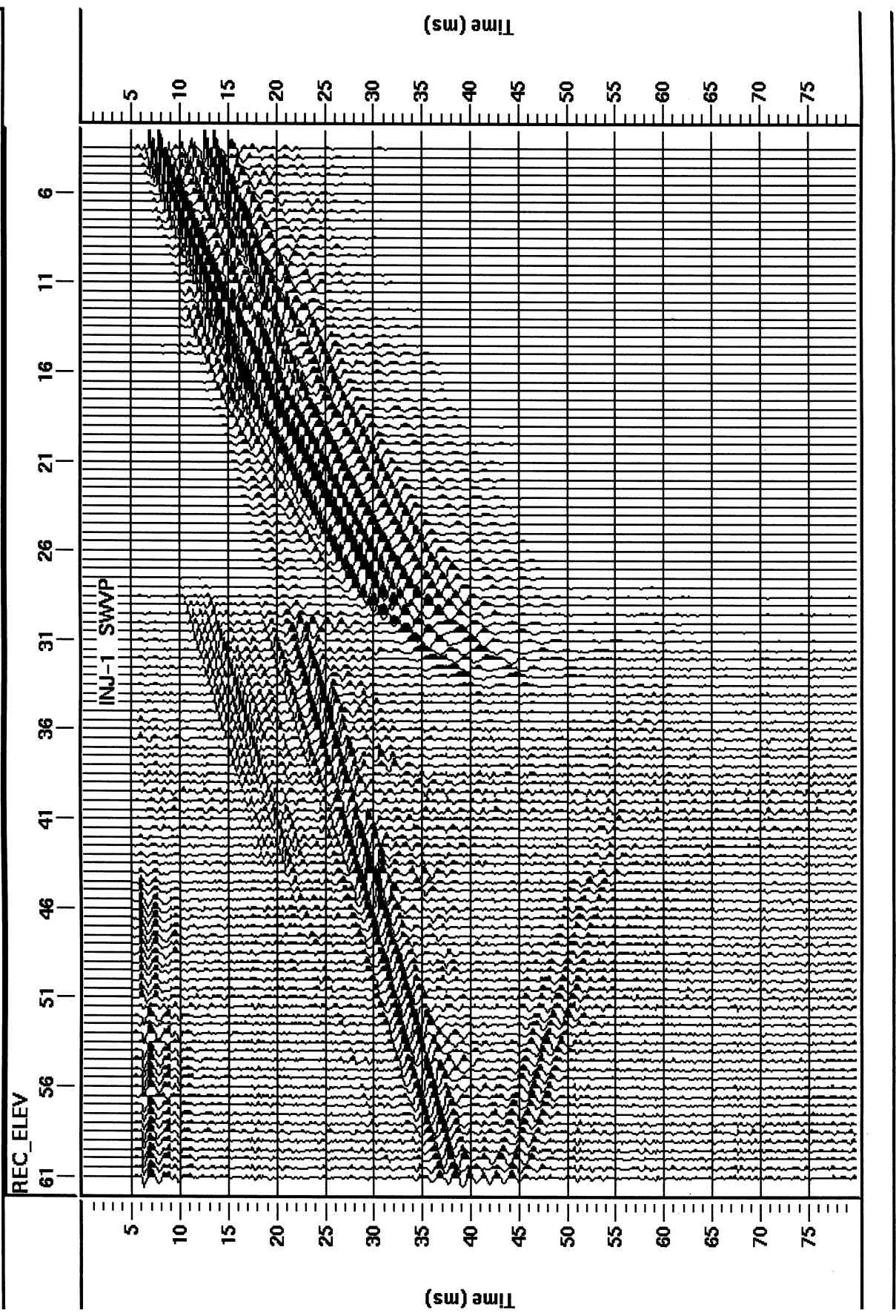


Figure 18. Single well vertical profile of well INJ-1 showing P-wave (10-30 ms) and tube-wave (5-40 ms). The receiver depth is labeled as rec_elev in meters..

LBNL Piezoelectric Source

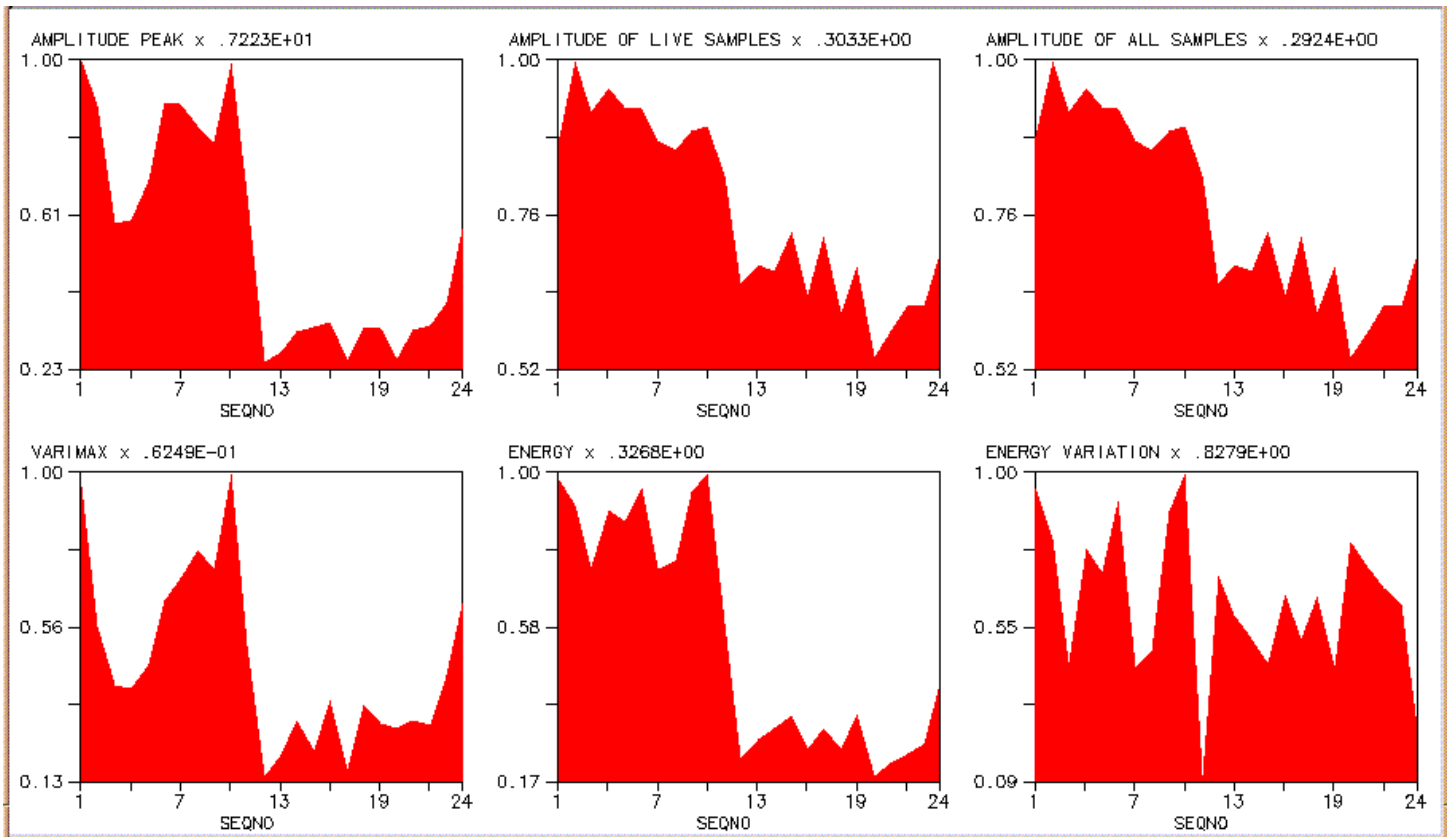


Figure 19. Amplitude analysis using various measures of the 24 hydrophones in the receiver well for a single shot gather using the LBNL piezoelectric source with a 4 kV pulse.

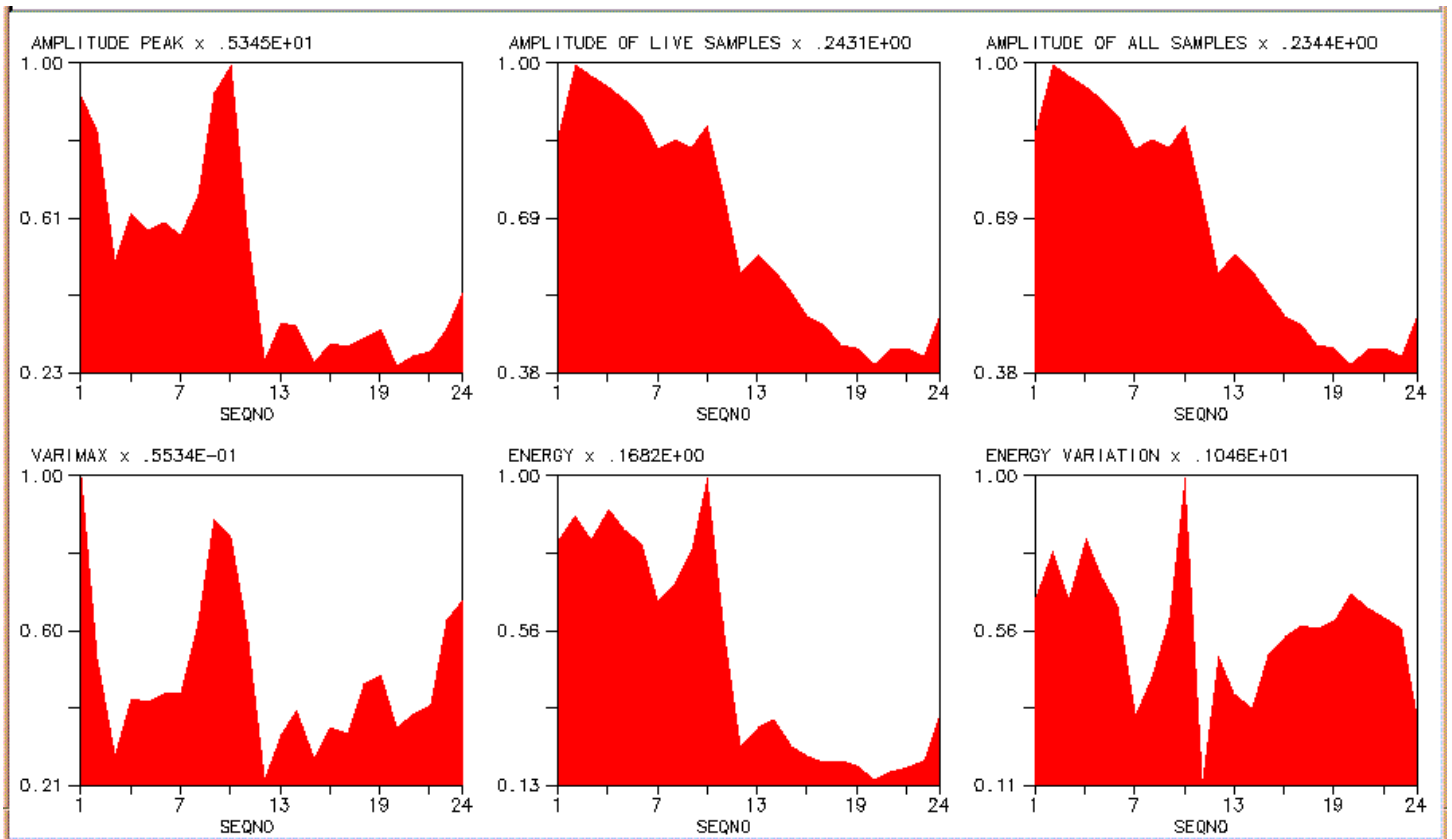


Figure 20. Amplitude analysis using multiple measures of the LBNL POV source for 24 hydrophones in a crosswell acquisition geometry. The source used a 4 kV pulse.